Journal of Chemical Crystallography (2019) 49:29–36
https://doi.org/10.1007/s10870-018-0747-x

ORIGINAL PAPER

Crystal and Molecular Structure and DFT Calculations of the Steroidal Oxime 6*E*-Hydroximino-androst-4-ene-3,17-dione ($C_{19}H_{25}NO_3$) a Molecule with Antiproliferative Activity

Rex A. Palmer[1] · David R. Lisgarten[2] · Jeremy K. Cockcroft[3] · John N. Lisgarten[4] · Rosemary Talbert[2] · Trevor Dines[5] · Ranju Bansal[6] · Pratap Chandra Acharya[7] · Amruta Suryan[6]

Received: 9 September 2017 / Accepted: 26 October 2018 / Published online: 9 November 2018

Abstract

The single crystal X-ray structure of the novel steroid derivative, 6*E*-hydroximino-androst-4-ene-3,17-dione ($C_{19}H_{25}NO_3$) (code name RB-499), possessing antiproliferative activity against various cell lines is presented. The analysis produced the following results: chemical formula $C_{19}H_{25}NO_3$; Mr = 315.40; crystals are orthorhombic space group $P2_12_12_1$ with Z = 4 molecules per unit cell with a = 6.2609(2), b = 12.5711(4), c = 20.0517(4) Å, Vc = 1578.18(7) Å^3, crystal density Dc = 1.327 g/cm³. Structure determination was performed by direct methods, Fourier and full-matrix least-squares refinement. Hydrogens were located in the electron density and refined in position with isotropic thermal parameters. The final R-index was 0.0324 for 3140 reflections with $I > 2\sigma$ and 308 parameters. The Absolute Structure Parameter − 0.07(5) confirms the correct allocation of the absolute configuration. The presence of the double bond C=O at position 3 in Ring A has caused a distortion from the usual chair conformation and created an unusual distorted sofa conformation folded across an approximate m-plane through C(1)–C(4). Ring B is a distorted chair, its conformation being influenced by the presence of the C(6)=N(6)–O(6)H group in position 6. Ring C is a symmetrical chair. Ring D exhibits both a distorted mirror symmetry conformation [influenced by the C(17)=O(17) group] and a distorted twofold conformation. DFT calculations indicated some degree of flexibility in rings A, C and D with ring A showing the greatest variation in torsion angles. The crystal packing is governed by H-bonds involving O(3), O(6) and O(17). DFT calculations of bond distances and angles, optimized at the B3LYP/6–31++G(d,p) level, were in good agreement with the X-ray structure.

Electronic supplementary material The online version of this article (https://doi.org/10.1007/s10870-018-0747-x) contains supplementary material, which is available to authorized users.

✉ Rex A. Palmer
rex.palmer@btinternet.com

[1] Department of Crystallography, Biochemical Sciences, Birkbeck College, University of London, Malet Street, London WC1E 7HX, UK

[2] Biomolecular Research Group, School of Human and Life Sciences, Canterbury Christ Church University, North Holmes Road, Canterbury, Kent CT1 1QU, UK

[3] Department of Chemistry, University College London, Gower Street, London WC1E 6BT, UK

[4] School of Science, University of Greenwich (Medway Campus), Chatham Maritime, Kent ME4 4TB, UK

[5] Carnegie Laboratory of Physics, University of Dundee, Dundee DD1 4HN, UK

[6] University Institute of Pharmaceutical Sciences, Panjab University, Chandigarh 160014, India

[7] Department of Pharmacy, Tripura University (A Central University), Suryamaninagar, Tripura (W) 799022, India

Graphical Abstract

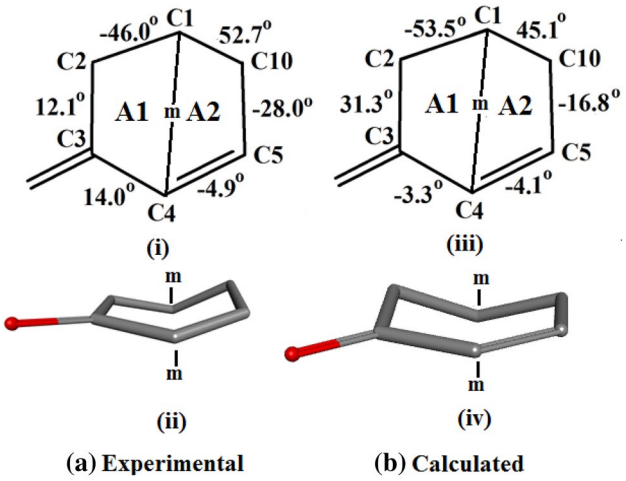

Ring A conformations: (a) Experimental and (b) Calculated. The differences in torsion angle values indicate a degree of flexibility in the ring. The ring conformations are shown in Figures (ii) and (iv) respectively (drawn with BIOVIA [12]. Regions A1 and A2 are approximately planar in both, being planar within 0.048 Å and 0.105 Å respectively.

Keywords Steroidal oximes · Cytotoxic steroids · Antiproliferates · Crystal structure · X-ray crystallography · DFT calculations

Introduction

Steroidal oximes have emerged as a new class of anticancer agents with either endocrine activity against aromatase and 5α-reductase enzymes or direct cytotoxicity on human cancer cells [1, 2]. Particular attention has been made to study the effect of 6*E*-hydroximinoandrostene framework on the antineoplastic activity [2–4]. However, during the synthesis the oximes tend to form the mixture of *Z* and *E*-geometrical isomers. The isolation and characterization of the desired *E*-isomer possesses greater challenge as the isomeric purity can affect the biological activity [4]. However, the present steroidal hydroximinoandrostene derivative was obtained as the pure *E*-isomer by recrystallization from methanol and the configuration of the title derivative was determined based on ^{1}H NMR studies [2]. Therefore, in this paper we have reported the crystal structure of 6*E*-hydroximino-androst-4-ene-3,17-dione in order to determine the isomeric orientation and other structural features.

Experimental

Synthesis and Crystallization

The compound was synthesized by the previously reported method and recrystallized in the form of yellow needles using methanol to obtain single crystals suitable for X-ray data collection [2].

X-Ray Data Collection and Results

A suitable crystal was selected and mounted on a SuperNova, Dual, Cu at zero, Atlas diffractometer. The crystal was flash frozen and kept at 150(2) K during data collection. Data collection was carried out using monochromated CuKα radiation on a (SuperNova Cu X-ray Source). Data were processed during data collection with the program CrysAlisPro, Agilent Technologies Version 1.171.36.28. The crystal showed excellent diffraction quality and no variation in intensity during the course of data collection. A total of 16,915 integrated reflections were collected, reducing to a data set of 3140 [R (int) = 0.0232], and completeness of data to theta = 67.684° of 99.7%. Further details of the crystal data are in Table 1. The chemical formulae and atom numbering scheme are given in Fig. 1a.

Structure Solution and Refinement

Initially using the program Olex2 [7] the structure was solved with the ShelXS [8] structure solution program using direct methods and refined with the ShelXL [9] refinement package using full matrix least squares minimization. Further refinement was subsequently carried out as follows. All H atoms were deleted and after further cycles of anisotropic refinement involving the non-H atoms a SHELXL [9] difference electron density plot was examined. The strongest peaks located in geometrically acceptable positions as H atoms were refined in position with isotropic thermal

Table 1 Crystal data and structure refinement for Ranju_exp_981 xstr0693

Identification code	Ranju_exp_981 xstr0693
Empirical formula	$C_{19}{\cdot}H_{25}{\cdot}N{\cdot}O_3$
Formula weight	315.40
Temperature	150(2) K
Wavelength	1.54184 Å
Crystal system	Orthorhombic
Space group	P $2_12_12_1$
Unit cell dimensions	a = 6.2609(2) Å α = 90° b = 12.5711(4) Å β = 90° c = 20.0517(4) Å γ = 90°
Volume	1578.18(7) $Å^3$
Z	4
Density (calculated)	1.327 Mg/m^3
Absorption coefficient	0.712 mm^{-1}
F(000)	680
Crystal size	0.426 × 0.340 × 0.233 mm^3
Theta range for data collection	4.151–73.616°
Index ranges	$^-$7 <= h <= 7 $^-$15 <= k <= 15 $^-$17 <= l <= 24
Reflections collected	16,915
Independent reflections	3140 [R(int) = 0.0232]
Completeness to theta = 67.684°	99.7%
Refinement method	Full-matrix least-squares on F2
Data / restraints / parameters	3140/0/308
Goodness-of-fit on F2	1.056
Final R indices [I > 2sigma(I)]	R1 = 0.0324, wR2 = 0.0870
R indices (all data)	R1 = 0.0326, wR2 = 0.0873
Absolute structure parameter	$^-$0.07(5)
Extinction coefficient	N/A
Largest diff. peak and hole	0.239 and −0.185 e.$Å^{-3}$

parameters. All H atoms in the structure were located during this procedure. Final X-ray refinement was carried out using SHELXL [9] implemented in the WinGX system of programs [10]. Geometrical calculations were made with the programs PARST and PLATON [11] as implemented in WinGX. In the final refinement cycle there were 3140 data to 308 parameters, resulting in a final goodness-of-fit on F2 of 1.056. Final R indices for [I > 2 sigma (I)] were R1 = 0.0324, wR2 = 0.0870 and R indices (all data) R1 = 0.0326, wR2 = 0.0873. The largest and smallest difference electron density regions were + 0.239 and − 0.185 e$Å^{-3}$, respectively. Full crystal data is available in the Supplementary Tables.

Discussion of the Crystal Structure

Figure 1a shows the chemical formula and atom numbering scheme. Figure 1b and c are Ortep/Raster [5, 6] views of the molecule looking approximately perpendicular and edge on to the steroid skeleton respectively. The molecular packing in the crystal is illustrated in Fig. 7 drawn with MERCURY [12].

The molecular skeleton is predominantly flat. The overall deviation from planarity in combined rings A, B, C and D is 0.22 Å. Some flattening has occurred in ring A in the region of C(3)=O(3), in ring B in the region of C(6)=N(6) and in ring D in the region of C(17)=O(17). Consequently Rings A and D have adopted unusual conformations as described below. All bond lengths and angles conform to standard values [see the website CCDC MOGUL (https://www.ccdc.cam.ac.uk/solutions/csd-system/components/mogul/)]. The conformation of ring A is shown in Fig. 2. Atoms C(2), C(3), C(4), C(5) and C(10) form an approximately planar region with C(1) out of the plane forming an approximate sofa conformation. Ring B is a distorted chair (Fig. 3). Ring C is in a chair conformation (Fig. 4). The 5-membered ring D (Fig. 5) exhibits both a distorted mirror symmetry and a distorted twofold symmetry. With respect to 5-membered rings no alternative descriptions exist (ie sofa or half-chair). Hydrogen bonding is illustrated in Fig. 7 and Table 2 provides details of the hydrogen bond geometry involving the three oxygens. The geometry of the oxime moiety C(6)=N(6)–O(6)–H(6) is of particular interest. Figure 6 shows the bond lengths and angles for both the experimental and calculated oxime structures which show only small differences. The torsion angle τ = C(6)=N(6)–O(6)–H(6) has values of 171.38° in the experimental structure and 176.71° in the calculated structure indicating that the moiety is flatter in the calculated structure. The bond length C(6)=N(6) is 1.281(2) Å (experimental) and 1.284 Å (calculated) which is marginally short for this type of bond; bond N(6)–O(6) has values of 1.406(2) Å (experimental) and 1.405 Å (calculated) both of which correspond to the standard value for this type of bond. The bond lengths of the two C=O groups in the structure are also of interest and display values corresponding to the norm with C(3)=O(3) being 1.221(2) Å (experimental) and 1.220 Å (calculated) and C(17)=O(17) = 1.214(2) Å (experimental) and 1.207 Å (calculated). The equivalence of the C(3)=O(3) and C(17)=O(17) bond lengths is somewhat unexpected in view of the fact that O(17) participates in the molecular packing as a much stronger O–H–O hydrogen bond acceptor than O(3) (Table 2).

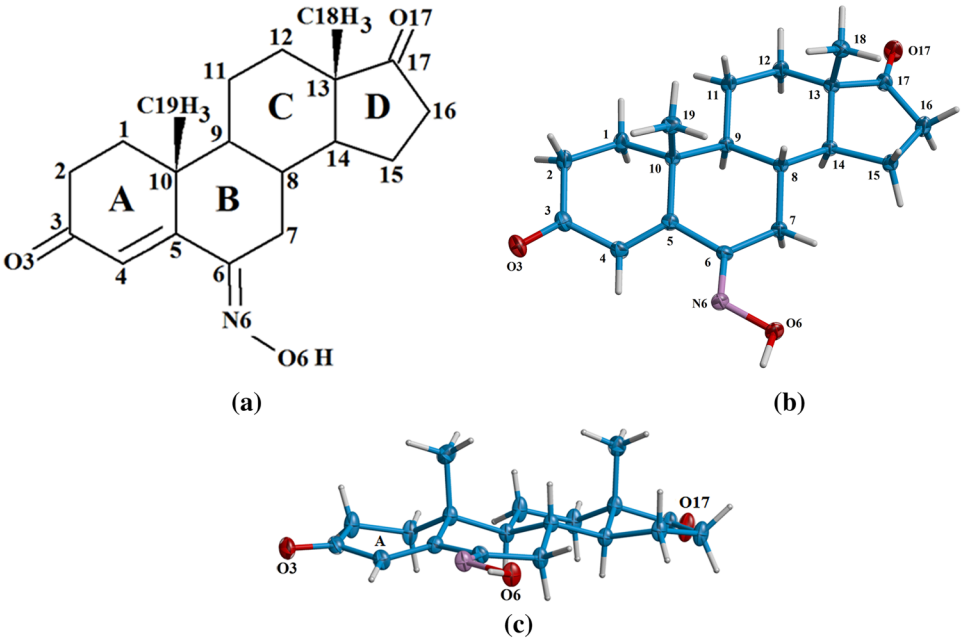

Fig. 1 **a** Atom numbering scheme and chemical formula. **b** View of the molecule including atom numbering scheme. Drawn with Ortep/Raster [5, 6]. Thermal ellipsoids are drawn at 60% probability. **c** Edge on view of the molecule. Thermal ellipsoids are drawn at 60% probability. Drawn with Ortep/Raster [5, 6]. Note the unusual conformation of Ring A

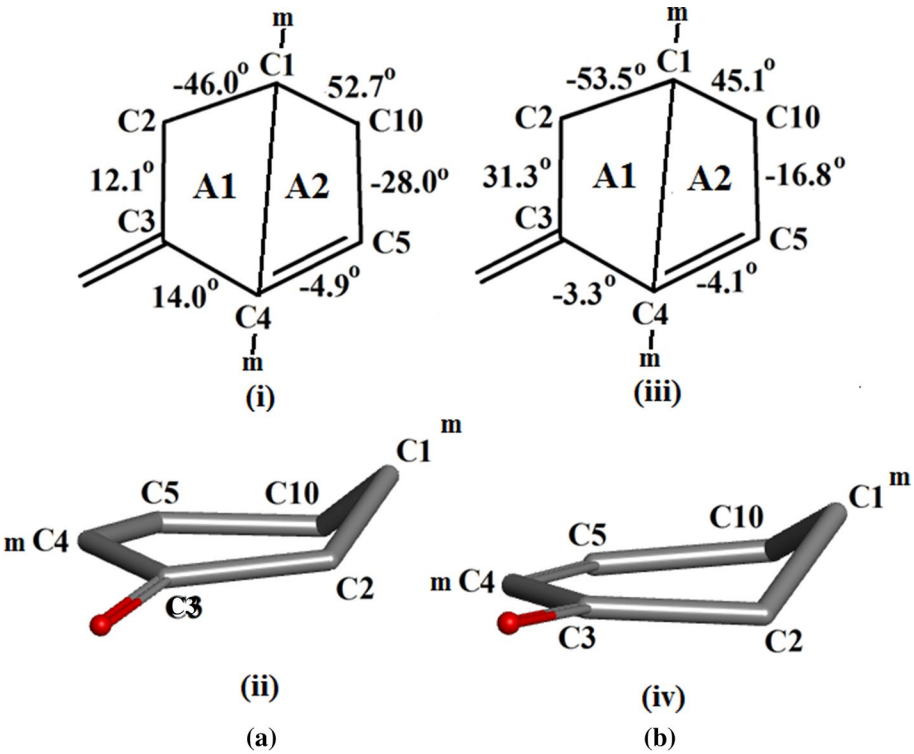

Fig. 2 Ring A conformations: **a** Experimental and **b** Calculated. The overall conformations appear to be similar whereas the torsion angle values indicate changes between the two. The ring conformations can be examined in (ii) and (iv) respectively (drawn with BIOVIA [13]). Regions C(2)–C(3)–C(4)–C(5)–C(10) are approximately planar in both, being planar within 0.048 and 0.105 Å respectively. There is an approximate m plane through C(2) and C(10). Atom C(1) is located significantly out of this plane. The overall conformation of ring A is thus a distorted sofa as can be seen in this figure. A different view of this unusual conformation in Ring A can also be seen clearly in Fig. 1c

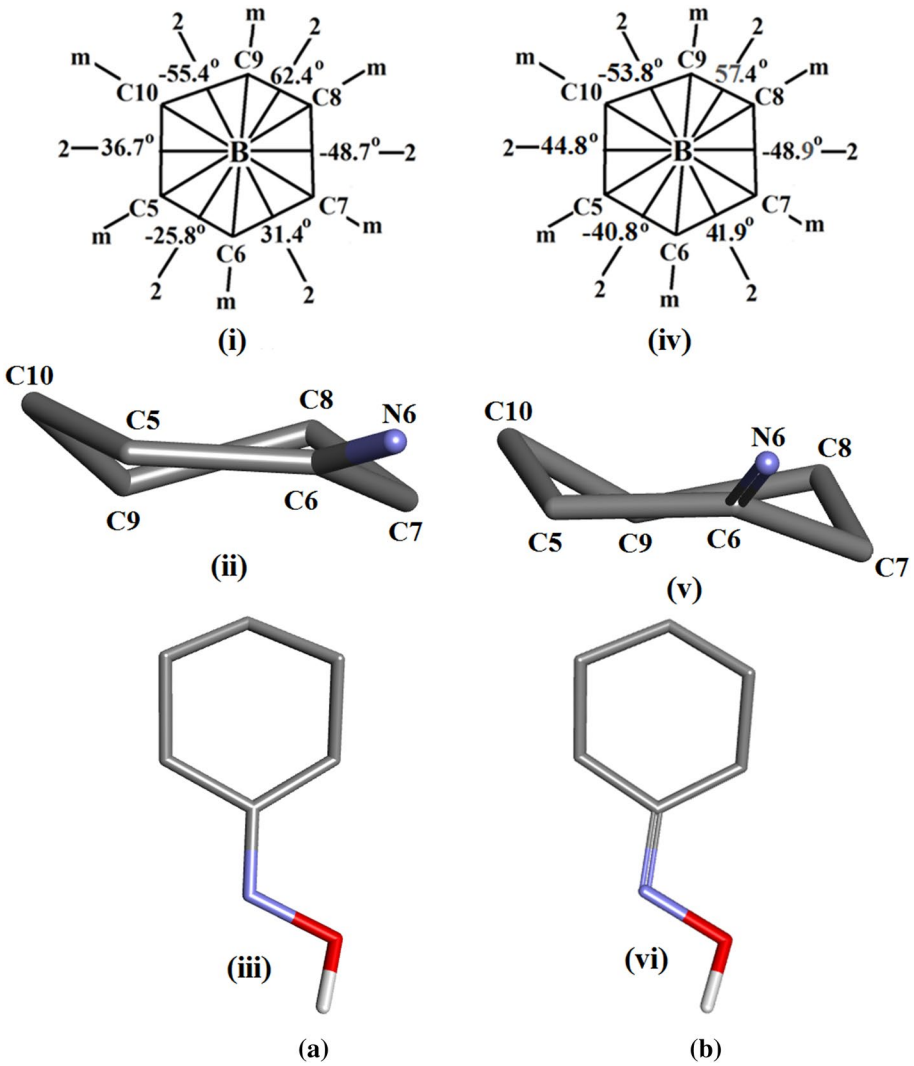

Fig. 3 Ring B conformation is a distorted chair in both the experimental and calculated structures. The ring torsion angles between experimental and calculated correspond more closely than those of ring A but there are still a number of significant differences : (i) and (iv) show the ring torsion angles, pseudo m-planes and twofold axes; (ii) and (v) show the conformations drawn with Biovia [13] looking down the pseudo twofold axis perpendicular to C(5)–C(6) and C(8)–C(9). (iii) and (vi) clearly show the close correspondence of the NOH side chain conformations also drawn with Biovia [13]

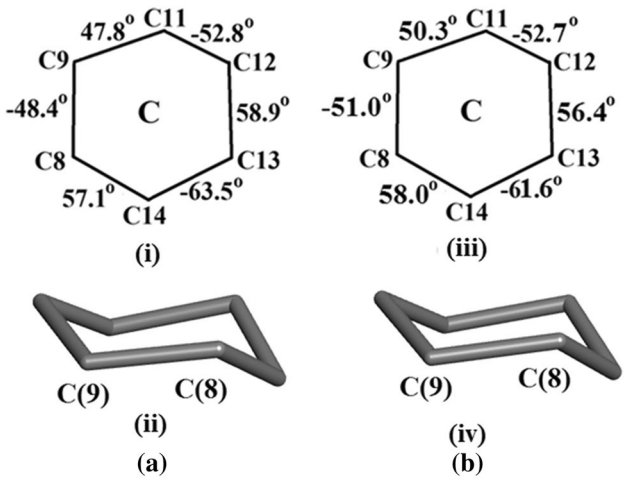

Fig. 4 The ring C conformation is a standard symmetrical chair in both the experimental and calculated structures. The ring torsion angles between experimental and calculated correspond closely: (i) and (iii) show the ring torsion angles; (ii) and (iv) show the conformations drawn with Biovia [13]

DFT Calculations

DFT calculations were performed with the *Gaussian 09* program [16], using the hybrid SCF-DFT method B3LYP, which incorporates Becke's three-parameter hybrid functional [14] and the Lee, Yang and Parr correlation functional [17], in conjunction with the 6-311++G(d,p) basis set [18]. Geometry optimization resulted in a structure for which the computed bond lengths and angles exhibit strong correspondence with the experimental structure. However corresponding torsion angles, as discussed below, in many cases exhibit significantly different values. A full listing of torsion angles for both structures is provided for comparison as an item in the Supplementary Information.

The conformations of Ring A observed in both the experimental and calculated structures are shown in Fig. 2. Both exhibit the unusual conformation involving two four component approximately planar regions which are approximately mirror related. Figure 3 shows the ring B distorted

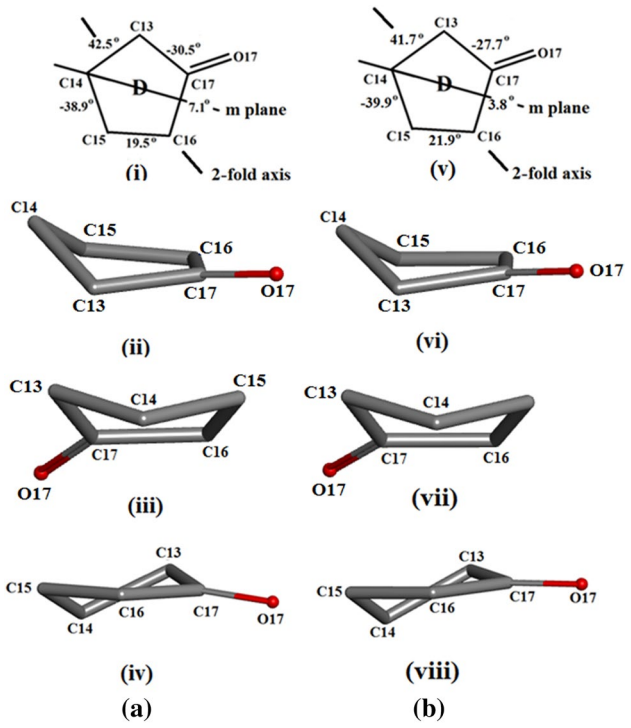

Fig. 5 The ring D conformation exhibits a distorted mirror symmetry in both the experimental and calculated structures. The ring torsion angles between experimental and calculated correspond closely: (i) and (v) show the ring torsion angles; (ii) and (vi) show the distorted mirror conformations side ways on and (iii) and (vii) are views which demonstrate the ring mirror symmetry drawn with Biovia [13]. There is a less symmetrical approximate twofold secondary ring shape in both shown in (iv) and (viii) respectively. The ring asymmetry parameters for mirror and two-fold symmetry respectively [14] are as follows: experimental $\Delta Cs(14) = 8.1$ (mirror), $\Delta C_2(16) = 15.0$ (twofold); calculated $\Delta Cs(14) = 4.3$ (mirror), $\Delta C_2(16) = 15.4$ (twofold). In both the experimental and calculated structure the envelope symmetry m is far closer than the symmetry 2. These results strongly suggest that ring D is subject to a degree of conformational flexibility. This may be an important factor with respect to the biological function

Table 2 Hydrogen bonds [Å and °]

D–H···A	d(D–H)	d(H···A)	d(D···A)	< (DHA)
O(6)–H(6)···O(17)#1	0.97(3)	1.77(3)	2.7382(17)	173(3)
C(2)–H(2B)···O(6)#2	0.97(3)	2.53(3)	3.436(2)	154.1(18)
C(7)–H(7B)···O(3)#3	0.99(3)	2.38(2)	3.217(2)	141.6(18)

Symmetry transformations used to generate equivalent atoms: #1 −x + 1/2, −y + 1, z−1/2 #2 −x + 1, y−1/2, −z + 1/2 #3 −x,y + 1/2, −z + 1/2

Note CH···O interactions as listed here may be considered to be weak Hydrogen bonds

chair conformations in both the experimental and calculated structures. The ring torsion angles between experimental and calculated structures correspond more closely than those of ring A but there are still a number of significant differences: (i) and (iv) show the ring torsion angles, pseudo m-planes and twofold axes; (ii) and (v) show the conformations drawn with Biovia [13] looking down the pseudo twofold axis perpendicular to C(5)–C(6) and C(8)–C(9). (iii) and (vi) clearly show the close correspondence of the NOH side chain conformations. The ring C conformation as shown in Fig. 4 is a standard symmetrical chair in both the experimental and calculated structures. The ring torsion angles between experimental and calculated correspond closely: (i) and (iv) show the ring torsion angles; (ii) and (v) show the conformations. The ring D conformations in the experimental and calculated structures are shown in Fig. 5. The predominant ring D conformation exhibits a distorted m-symmetry in both the experimental and calculated structures. The ring torsion angles between experimental and calculated correspond closely: (i) and (v) show the ring torsion angles; (ii) and (vi) show the distorted m-symmetry side ways on and (iii) and (vii) are views which demonstrate the distorted ring mirror symmetry drawn with Biovia [13]. There is a less symmetrical secondary distorted twofold ring shape in both shown in (iv) and (viii) respectively. The ring asymmetry parameters for mirror and two-fold symmetry respectively [19] are as follows: experimental $\Delta Cs(14) = 8.1$ (mirror), $\Delta C_2(16) = 15.0$ (twofold); calculated $\Delta Cs(14) = 4.3$ (mirror), $\Delta C_2(16) = 15.4$ (twofold). In both the experimental and calculated structure the sofa symmetry m is far closer than the symmetry 2 half-chair. These results strongly suggest that ring D is subject to a degree of conformational flexibility. This may be an important factor with respect to the biological function. Views of the Experimental and Calculated structures drawn with Biovia [13] can be seen in Fig. 8 which indicate both the overall similarity between the two and the minor but possibly biologically important differences.

Conclusions and Proposed Future Studies

Several X-ray crystallographic studies on the steroids have been performed in an attempt to understand the significance of preferred conformations, relative stabilities, and substituent influence with regard to the receptor interactions and other binding modes. Insight about the conformation of the A-ring as well as D-ring on the biological properties of the steroid has been provided by Duax and coworkers [15]. In

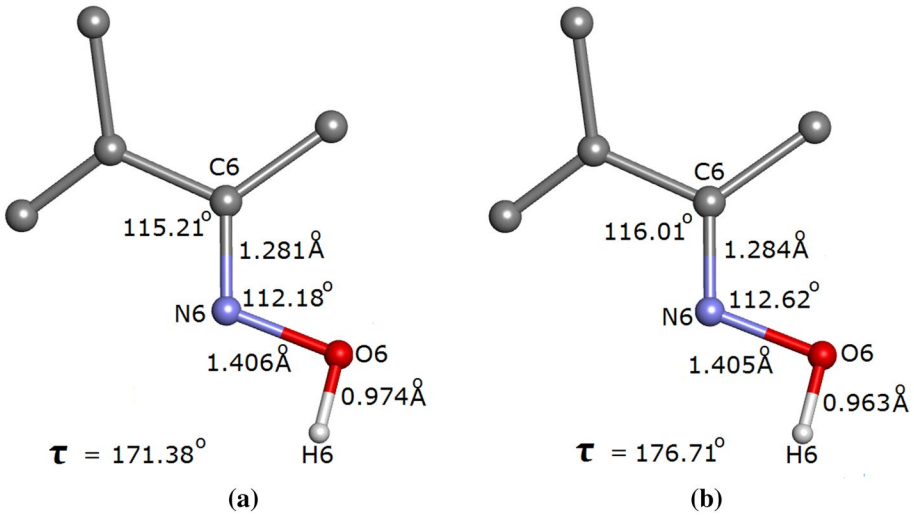

Fig. 6 The oxime moiety C6=N6–O6-H6 showing the geometry in **a** the experimental structure and **b** the calculated structure

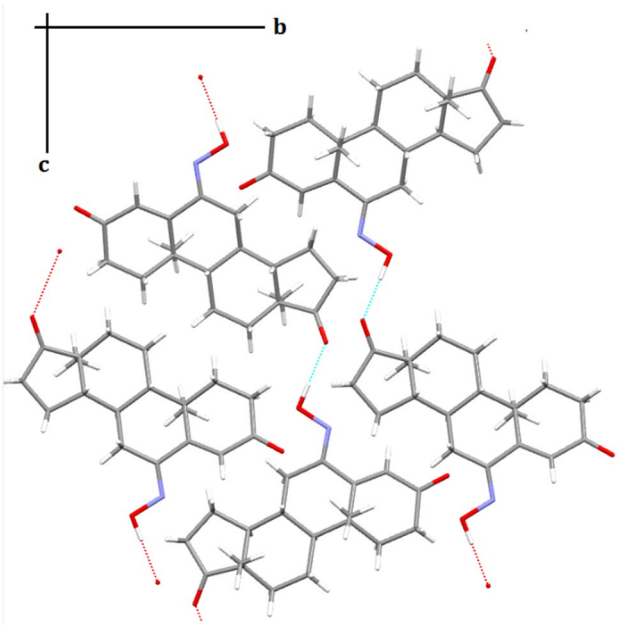

Fig. 7 Crystal packing down a. H-bonds are shown as red or blue lines. Drawn with MERCURY [15]. (Color figure online)

general, similarities in the A-ring region and dissimilarities in the D-ring region were observed when the structures of agonists and antagonists of specific steroid hormones were compared. It is suggested that the steroid A-ring bears responsibility for receptor binding while the D-ring controls expression of activity. A detailed overview of the *molecular structure and biological activity of steroids* has recently been published [20]. The present high resolution X-ray structure revealed an unusual Ring A conformation associated with the double bond C(4)=C(5). Subsequent DFT calculations indicated a degree of flexibility in Ring A and to a lesser extent in Ring D. It is possible that these effects may have an influence on the receptor binding properties of the molecule. A search is currently being made for biological receptors with known structures to which binding may occur. This will hopefully lead to further studies both in vitro and computer based with a view to ultimately designing new compounds with improved antiproliferative activity. In another area of therapeutic interest, two recent studies involving biomedical-steroid function, promise to lead to interesting structure function studies. It was shown that 16,17-pyrazoline substituted heterosteroids [21] and 16-arylideno steroids [22] both represent a new class of neuroprotective agents for the treatment of Alzheimer's and Parkinson's diseases. In particular it was shown that the introduction of a pyrazoline ring at the 16,17 position of the steroid skeleton resulted in improvement of neuroprotective effects. These steroids significantly lowered the enhanced TNF-α levels. It may be possible in future to rationalize these findings through computer based drug-receptor binding studies.

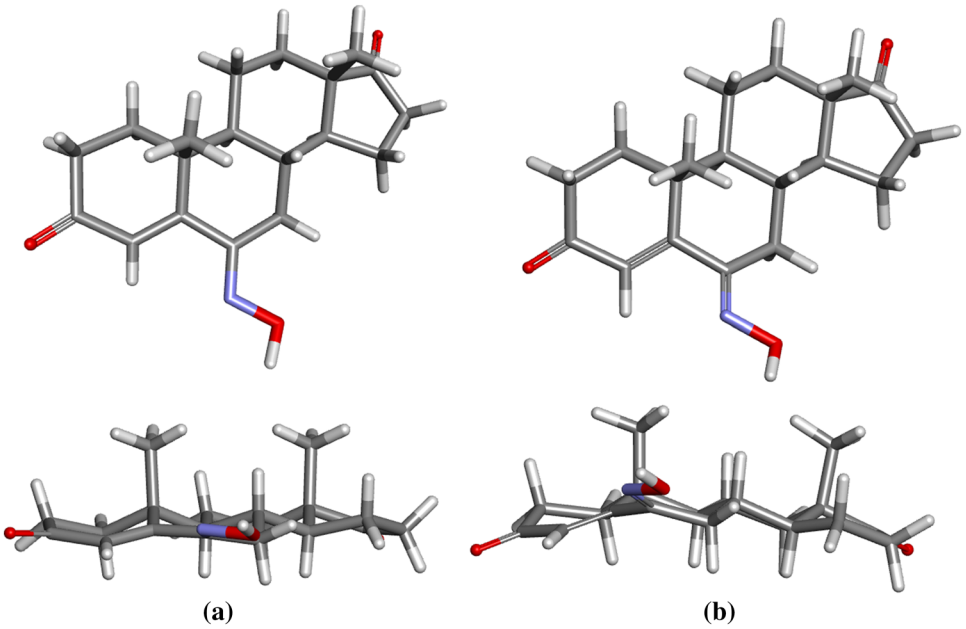

Fig. 8 Views of the **a** experimental and **b** calculated structures drawn with Biovia [13]

Acknowledgements We acknowledge financial support from the EPSRC for funding the X-ray diffractometers (Grant Reference EP/K03930X/1).

References

1. Bansal R, Acharya PC (2014) Chem Rev 114:6986–7005
2. Acharya PC, Bansal R (2014) Arch Pharm Chem Life Sci 347:193–199
3. Jaime R, Lucia N, Solange P, Carlos J (1997) Tetrahedron Lett 38:1833–1836
4. Deive N, Rodriguez J, Jimenez C (2001) J Med Chem 44:2612–2618
5. C. L.Barnes (1997) J Appl Cryst 30:568 [Based on ORTEP-III (v 1.0.3) by Johnson CK and M. N. Burnett]
6. Merrit EA, Bacon DJ (1997) Meth Enzymol 277: 505. [Implemented in WinGX(qv) and generated by Ortep-III for Windows]
7. Dolomanov OV, Bourhis LJ, Gildea RJ, Howard JAK, Puschmann H (2009) J Appl Crystallogr 42:339–341
8. Sheldrick GM (2008) Acta Crystallogr Sect A 64:112–122
9. SHELXL-2014 [As implemented in WinGX (8)]
10. Farrugia LJ (1999) J Appl Crystallogr 32:837–838
11. Spek AL (1990) Acta Crystallogr Sect A 46:C34
12. Bruno IJ, Cole JC, Edgington PR, Kessler MK, Macrae CF, McCabe P, Pearson J, Taylor R (2002) Acta Cryst B58:389
13. Dassault Systèmes BIOVIA (2016) Discovery studio modeling environment, release 2017. Dassault Systèmes, San Diego
14. Becke AD (1993) J Chem Phys 98:5642–5648
15. Duax WL, Griffin JF, Rohrer DC, Swenson DC, Weeks CM (1981) J Steroid Biochem 15:41–47
16. Frisch MJ, Trucks GW, Schlegel HB et al Gaussian 09, Revision A.1, Gaussian, Inc., Wallingford, CT, 2009
17. Lee C, Yang W, Parr RG (1988) Phys Rev B 37:785–789
18. Binkley JS, Seeger R, Pople JA (1980) J Chem Phys 72:650
19. Duax WL, Norton DA (1975) Atlas of Steroid structure. FI/Plenum Data Co., New York
20. Bohl M (2018) Molecular structure and biological activity of steroids. In: M. Bohl, W.L. Duax (eds.) CRC press
21. Singh R, Thota S, Bansal R (2018) Studies on 16,17-pyrazoline substituted heterosteroids as anti-Alzheimer and anti-Parkinsonian agents using LPS induced neuroinflammation models of mice and rats. ACS Chem Neuroscie 9(2):272–283
22. Singh R, Bansal R (2017) Investigations on 16-arylideno steroids as a new class of neuroprotective agents for the treatment of Alzheimer's and Parkinson's diseases. ACS Chem Neuroscie 8(1):186–200